polymorphism of the *HtrA2/Omi* gene was also shown to be associated with PD. These data suggest that HtrA2/Omi is a susceptible factor for PD (PARK13 locus) (30). The results from the targeted disruption of HtrA2/Omi in mice and a mutation screening for HtrA2/Omi in humans suggest that a loss of the function of HtrA2/Omi may be involved in the pathogenesis of PD, but the relationship between HtrA2/Omi and PD remains unclear. In the present study, we performed immunohistochemical studies on HtrA2/Omi using autopsied brains from patients with α-synucleinopathies, including PD. We investigated the detailed neuroanatomic localization of HtrA2/Omi in these diseased brains and found strong HtrA2/Omi immunoreactivity in the α-synuclein-containing inclusions in PD, DLB, and MSA.

MATERIALS AND METHODS

Tissue Preparation

Brains from autopsies of 8 control subjects without any neurologic abnormalities (age range, 54–78 years; mean, 68.4 years; 6 men and 2 women), 10 patients with PD (age range, 66–90 years; mean, 77.5 years; 6 men and 4 women), 5 patients with DLB (age range, 69–86 years; mean, 74.8 years; 4 men and 1 woman), 10 patients with MSA (age range, 52–78 years; mean, 69.1 years; 4 men and 6 women), 5 patients with Alzheimer disease (AD) (age range, 67–85 years; mean, 75.2 years; 1 man and 4 women), a patient with frontotemporal dementia with parkinsonism linked to chromosome 17 (54-year-old man), and a patient with frontotemporal lobar degeneration with ubiquitin-positive inclusions (66-year-old woman). These materials were selected from the brain banks at the Neuropathology Laboratories of Kyoto University and Medical University of Vienna. In 5 of 10 patients with MSA, the MSA was classified as cerebellar variant, and in the other 5 patients, MSA of the parkinsonian variant. The clinical profiles from all cases are summarized in Table 1. All brains were fixed in 10% neutral formalin for about 2 weeks at room temperature. Several paraffin-embedded tissue blocks, including the frontal and temporal cortices, basal ganglia, brainstem, and cerebellum, were prepared and cut into 6-μm-thick sections on a microtome. Sections were deparaffinized in xylene, followed by rehydration in a decreasing concentration of ethanol solutions. For routine pathologic evaluation, the sections from all cases were stained with hematoxylin and eosin (H&E), Klüver-Barrera, and modified Bielschowsky methods. No histologic abnormalities were detected in the sections from any of the control cases. A loss of dopaminergic neurons associated with the presence of classic (brainstem-type) LBs was observed in the substantia nigra from both PD and DLB cases. In addition, many cortical LBs were found in the cerebral cortical regions of the DLB cases, and diagnoses of DLB cases were made according to revised criteria (31). Numerous GCIs were detected in the sections from all of the MSA cases.

Immunohistochemistry

To examine the immunohistochemical localization of HtrA2/Omi, we used an anti-HtrA2/Omi anti-serum raised by immunizing rabbits with *Escherichia coli* expressing the C-terminal His_6-tagged mature form of human HtrA2/Omi protein (22). The deparaffinized sections were pretreated with 0.3% hydrogen peroxide (Santoku, Tokyo, Japan) in

TABLE 1. Case Materials

Case	Age, year/ Sex	Major Diagnosis	Duration of Neurologic Illness, year/Postmortem Delay, hour
Control 1	62/M	Pancreatic carcinoma	NA/3.0
Control 2	68/M	Rheumatoid arthritis	NA/2.0
Control 3	73/M	Hepatocellular carcinoma	NA/4.5
Control 4	68/F	Breast cancer	NA/2.5
Control 5	75/M	Pulmonary emphysema	NA/2.0
Control 6	69/M	Lung cancer	NA/UD
Control 7	54/M	Pneumonia	NA/2.0
Control 8	78/F	Chronic renal failure	NA/9.8
PD 1	90/F	PD	9/2.0
PD 2	76/M	PD	14/2.5
PD 3	79/F	PD	13/1.5
PD 4	81/F	PD	8/2.5
PD 5	74/M	PD	20/UD
PD 6	66/M	PD	10/2.3
PD 7	76/M	PD	8/1.3
PD 8	88/M	PD	10/2.1
PD 9	67/M	PD	17/UD
PD 10	78/F	PD	11/12.0
DLB 1	81/M	DLB	UD/9.0
DLB 2	69/M	DLB	9/11.5
DLB 3	69/F	DLB	27/1.0
DLB 4	69/M	DLB	2/7.5
DLB 5	86/M	DLB	3/5.3
MSA 1	78/M	MSA-C	7/4.8
MSA 2	66/M	MSA-C	4/3.5
MSA 3	72/F	MSA-C	5/2.0
MSA 4	78/M	MSA-C	3/1.8
MSA 5	67/F	MSA-C	2/UD
MSA 6	52/F	MSA-P	3/2.5
MSA 7	77/F	MSA-P	5/1.4
MSA 8	69/F	MSA-P	8/6.1
MSA 9	72/F	MSA-P	12/1.2
MSA 10	60/M	MSA-P	6/3.5
OD 1	80/F	AD	UD/UD
OD 2	85/M	AD	10/UD
OD 3	67F	AD	5/4.2
OD 4	77/F	AD	9/1.4
OD 5	67/F	AD	8/5.9
OD 6	54/M	FTDP-17	8/6.0
OD 7	66/F	FTLD-U	UD/2.9

PD, Parkinson disease; DLB, dementia with Lewy bodies; MSA, multiple-system atrophy; OD, other disease; M, male; F, female; MSA-C, MSA of the cerebellar variant; MSA-P, MSA of the parkinsonian variant; AD, Alzheimer disease; FTDP-17, frontotemporal dementia with parkinsonism linked to chromosome 17; FTLD-U, frontotemporal lobar degeneration with ubiquitin-positive inclusions; NA, not applicable; UD, undetermined.

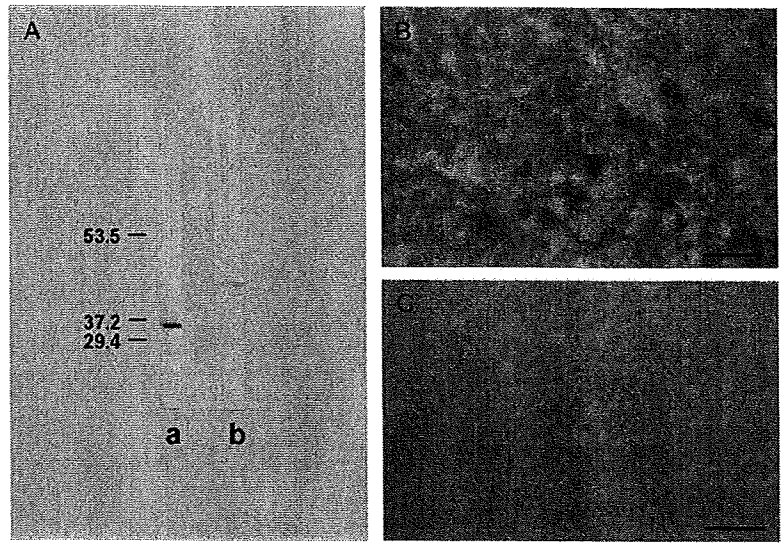

FIGURE 1. Characterization of anti-HTrA2/Omi anti-serum. **(A)** Western blot analysis of normal human brain homogenate. Membranes were incubated with the anti-HtrA2/Omi anti-serum (a) or preimmune serum (b) (see Materials and Methods). The molecular weights (in kilodaltons) are shown to the left. **(B, C)** Immunoreactivities in 20-μm cryosections of frontal cortices of wild-type control **(B)** and knockout **(C)** mice. Scale bars = 50 μm.

0.1 M phosphate-buffered saline (PBS) for 30 minutes at room temperature to inhibit endogenous peroxidase activity. After washing with 0.1 M PBS, the sections were blocked with 0.1 M PBS with 3% skim milk for 2 hours at room temperature. After rinsing with 0.1 M PBS, the anti-HtrA2/Omi anti-serum diluted in 0.1 M PBS (1:200) was applied onto the sections, and they were incubated at room temperature overnight in a humidified chamber. After washing with 0.1 M PBS, the sections were reacted with a biotinylated anti-rabbit immunoglobulin G (IgG; Vector Laboratories, Burlingame, CA) diluted in 0.1 M PBS (1:200) for 1 hour at room temperature, followed by incubation with an avidin-biotin-peroxidase complex (ABC) kit (Vector Laboratories) diluted in 0.1 M PBS (1:400) for 1 hour at room temperature. After rinsing with 0.1 M PBS and then 0.05 M Tris-HCl (pH 7.6), the sections were developed in a colorizing solution containing 0.02% diaminobenzidine tetrahydrochloride (Dojin, Kumamoto, Japan), 0.6% ammonium nickel (II) sulfate (Wako, Osaka, Japan), and 0.005% hydrogen peroxide in 0.05 M Tris-HCl (pH 7.6) for 10 minutes at room temperature. Some H&E-stained sections with classic or cortical LBs were photographed, decolorized with 70% ethanol and were then immunostained with the anti-HtrA2/Omi anti-serum using the ABC method described above. As a negative immunohistochemical control, some sections were incubated with a preimmune rabbit serum; no specific staining was detected in these control sections (data not shown).

Double Immunofluorescence Staining

To compare the anatomic distribution of α-synuclein-immunopositive inclusions to that of HtrA2/Omi-immunopositive inclusions in brains with α-synucleinopathies, we performed double-labeling immunohistochemistry using a goat polyclonal anti-α-synuclein antibody (sc-7011; Santa Cruz Biotechnology, Santa Cruz, CA) and the rabbit anti-HtrA2/Omi anti-serum. Some sections from the PD, DLB, and MSA cases were incubated with the combination of the anti-α-synuclein antibody (1:1000) plus the anti-HtrA2/Omi anti-serum (1:200) in 0.1 M PBS at room temperature overnight. After washing with 0.01 M PBS, the sections were reacted with

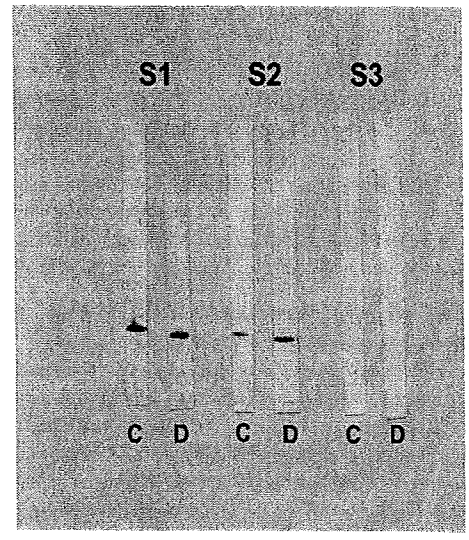

FIGURE 2. Western blot analysis of human brain fractions from control (C) and dementia with Lewy bodies (D) cases. All lanes were incubated with the anti-HtrA2/Omi anti-serum. S1, S2, and S3 indicate phosphate-buffered saline-soluble, sodium dodecyl sulfate-soluble, and formic acid-soluble fractions, respectively.

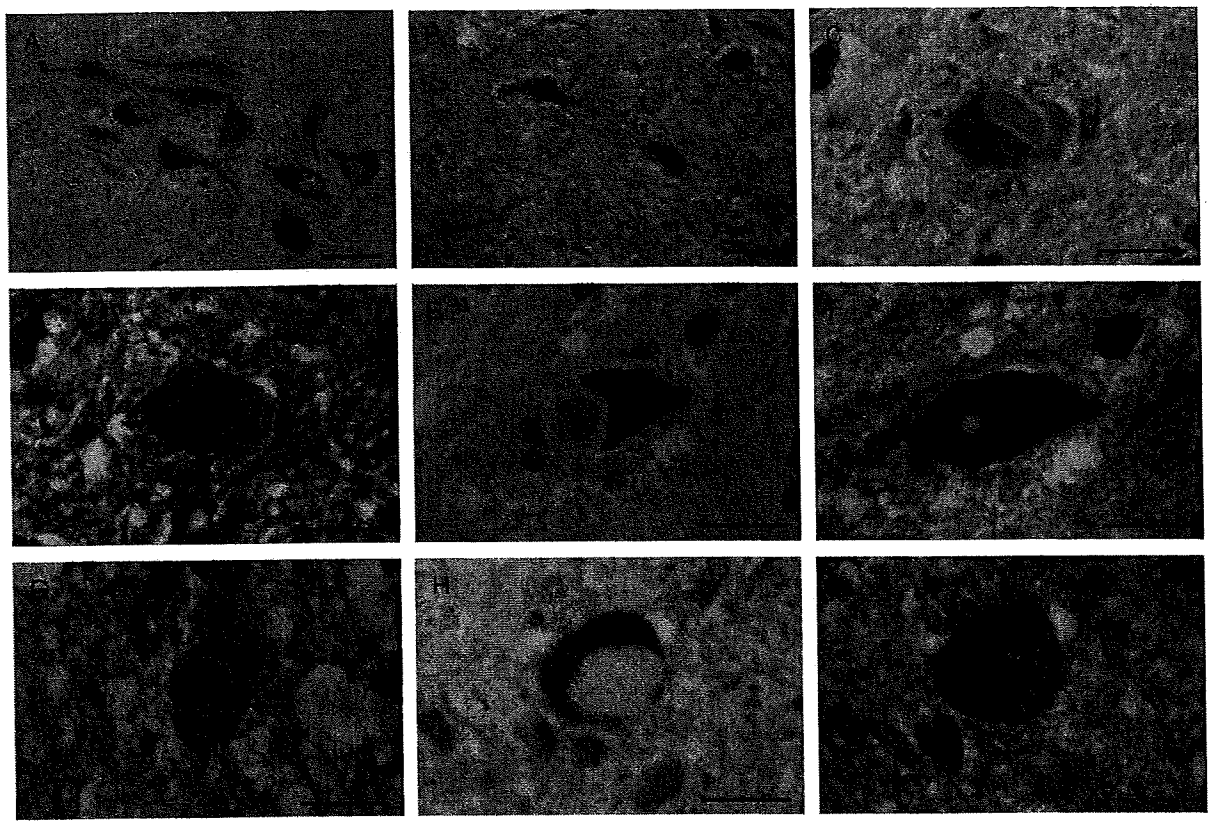

FIGURE 3. Substantia nigra sections stained with H&E and immunostained with the anti-HtrA2/Omi anti-serum. There is a similar immunolabeling pattern in the melanin-containing neurons in the control case **(A)** and in the Parkinson disease (PD) case **(B)**. Classic Lewy bodies (LBs) **(C, E)** show ring-shaped HtrA2/Omi immunolabeling pattern **(D, F)**. The classic LBs in **(C)** and **(E)** are identical to those in **(D)** and **(F)**, respectively. One remaining neuron in a PD case contained an immunopositive large LB (large arrow) and an immunopositive small LB (small arrow) **(G)**. A large, eosinophilic pale body **(H)** is also intensely immunopositive for HtrA2/Omi **(I)**. The pale body in **H** was the same as the one in **I**. Cases illustrated: **A**: Control 3; **B**: PD 3; **C, D**: PD 6; **E, F**: PD 2; **G**: PD 5; **H, I**: PD 7. Scale bars = **(A, B)** 50 μm; **(C–I)** 20 μm.

secondary antibodies consisting of a tetramethylrhodamine-conjugated swine anti-rabbit IgG (DakoCytomation, Glostrup, Denmark) and a fluorescein isothiocyanate-conjugated swine anti-goat IgG (Biosource, Camarillo, CA). After rinsing with 0.01 M PBS, the slides were coverslipped with Vectashield (Vector Laboratories) and were then viewed with a fluorescence microscope system (BZ-9000, Keyence, Osaka, Japan).

Semiquantitative Assessment of HtrA2/Omi-Immunopositive LBs and GCIs

To evaluate the proportions of HtrA2/Omi-immunopositive classic LBs in the substantia nigra, locus ceruleus, dorsal motor nucleus of the vagus, and basal nucleus of Meynert, we prepared several kinds of sections double-immunostained with α-synuclein and HtrA2/Omi from all 10 PD cases. After counting the α-synuclein-immunopositive classic LBs in these areas, we counted the double-immunolabeled classic LBs in the same areas. We then calculated the percentage of HtrA2/Omi-immunopositive classic LBs in each section and the average percentages of HtrA2/Omi-positive classic LBs in the substantia nigra, locus ceruleus, dorsal motor nucleus of the vagus, and basal nucleus of Meynert.

To estimate the proportions of HtrA2/Omi-immunopositive cortical LBs in DLB and GCIs in MSA, we prepared double-immunostained sections with α-synuclein and HtrA2/Omi from all of the DLB and MSA cases. Using the same counting method, we calculated the average percentages of HtrA2/Omi-positive cortical LBs in the superior frontal, cingulate, insular, and parahippocampal cortices and the average percentages of HtrA2/Omi-positive GCIs in the internal capsule, putamen, middle cerebellar peduncle, and cerebellar white matter.

Characterization of the Primary Anti-Serum

The specificity of the anti-HtrA2/Omi anti-serum was confirmed by Western blotting using human brain homogenates. Fresh brain tissues were obtained from the frontal cortex of an autopsied normal subject (68-year-old man). These materials were homogenized in 3 volumes of ice-cold 10 mM PBS containing 1% Nonidet P-40 (Nacalai Tesque, Kyoto, Japan), 0.5% sodium deoxycholate (Difco, Detroit, MI), 0.1% sodium dodecyl sulfate (SDS; Nacalai Tesque), 0.01% phenylmethylsulfonyl fluoride (Nacalai Tesque), 3% aprotinin (Sigma, St Louis, MO), and 1 mM sodium orthovanadate (Sigma). The

homogenates were then centrifuged at 15,000 revolutions per minute (r.p.m.) for 15 minutes at 4°C, and the supernatants were then mixed with an equivalent volume of electrophoresis sample buffer containing 10% glycerol (Nacalai Tesque), 2% SDS, 5% 2-mercaptoethanol (Nacalai Tesque), and 0.00125% bromophenol blue (Nacalai Tesque) in 62.5 mM Tris-HCl (pH 6.8). All samples were then heated for 3 minutes at 100°C and then cooled to room temperature. A 10-μL aliquot of the sample was loaded onto each lane of Mini-Protean II Ready Gels J (Bio-Rad, Hercules, CA), electrophoresed at a constant voltage of 200 V, and then transferred onto polyvinylidene diflouride membranes (Bio-Rad) at a constant voltage of 100 V. After blocking the nonspecific reactions with 3% skim milk plus normal goat serum in 25 mM Tris-buffered saline (TBS), the membranes were incubated with the anti-HtrA2/Omi serum (1:5000) or preimmune serum (1:5000) in 25 mM TBS plus 3% skim milk for 4 hours at room temperature. After washing with 25 mM TBS containing 0.1% Tween 20 (Bio-Rad), the membranes were reacted with an alkaline phosphatase-labeled anti-rabbit IgG (Vector, 1:1000) in 25 mM TBS with 3% skim milk for 1 hour at room temperature. After rinsing with 25 mM TBS containing 0.1% Tween 20, the primary antibodies were visualized using a 5-bromo-4-chloro-3-indolyl-phosphate/nitroblue tetrazolium kit (Nacalai Tesque).

We also performed immunohistochemical studies on HtrA2/Omi using HtrA2/Omi knockout mouse brain sections as a negative control. Brain tissues of knockout and wild-type control mice (both of which have been previously described [29]) were fixed in 10% neutral formalin, stored in 20% sucrose in 0.1 M phosphate buffer, and then cut into 20-μm-thick sections on a freezing microtome. Free-floating sections were immunostained with the anti-HtrA2/Omi serum (1:5000) using the ABC method described above.

Brain Tissue Fractionation

Human brain homogenates were divided into 3 fractions based on their solubility in PBS, SDS, and formic acid. Fresh frontal cortical tissue samples from a control subject (68-year-old man) and a patient with DLB (77-year-old man) were homogenized in 3 volumes of ice-cold 10 mM PBS containing 1% Nonidet P-40, 0.5% sodium deoxycholate, 0.1% SDS, 0.01% phenylmethylsulfonyl fluoride, 3%

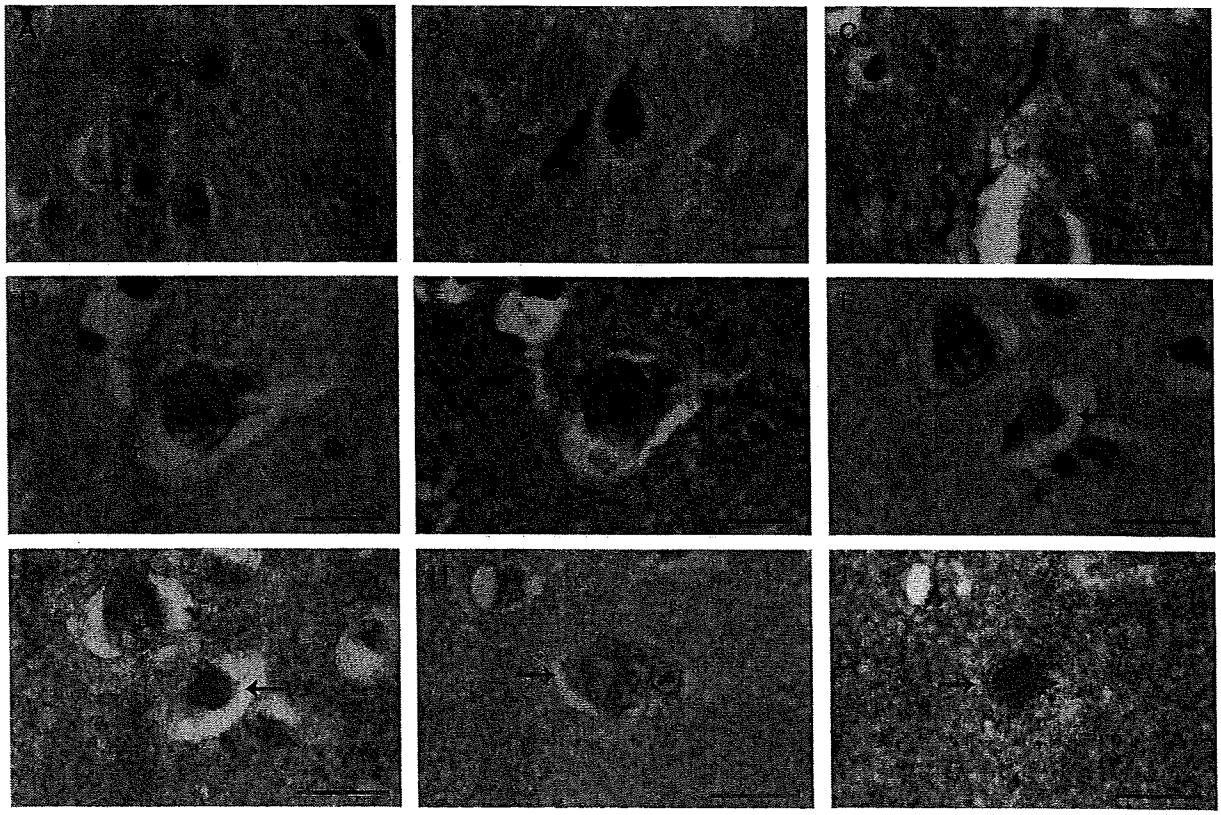

FIGURE 4. Cerebral cortical sections stained with H&E and immunostained with the anti-HtrA2/Omi anti-serum. In the hippocampus from normal controls, there was mild to moderate immunoreactivity in the pyramidal neurons, some of which had densely immunostained perinuclear regions **(A**, arrows**)**. In the hippocampus from patients with dementia with Lewy bodies (DLB), there was strong HtrA2/Omi immunoreactivity in some pyramidal neurons **(B)** and in a few Lewy neurites **(C)**. Cortical Lewy bodies (LBs) consisting of poorly defined, eosinophilic structures with no clear cores and halos **(D, F, H)** showed HtrA2/Omi immunoreactivity **(E, G, I)**. The cortical LBs (arrows) in **(D, F)** and **(H)** are the same as those in **(E, G)** and **(I)**, respectively. Cases illustrated: **A**: Control 4; **B, C, F, G**: DLB 1; **D, E**: DLB 2; **H, I**: DLB 5. Scale bars = 20 μm.

aprotinin, and 1 mM sodium orthovanadate. Each homogenate was centrifuged at 2,500 r.p.m. for 10 minutes at 4°C, and the supernatant was subsequently centrifuged at 55,000 r.p.m. for 1 hour at 4°C, yielding the supernatant (S1, PBS-soluble fraction) and pellet (P1). After washing with 10 mM PBS containing same additives (Buffer A), the P1 pellet was extracted with Buffer A containing 2% SDS and then centrifuged at 55,000 r.p.m. for 1 hour at 4°C, yielding the supernatant (S2, SDS-soluble fraction) and pellet (P2). After rinsing with Buffer A, the P2 pellet was extracted 70% formic acid and then centrifuged at 55,000 r.p.m. for 1 hour at 4°C. The formic acid extract was dried, and the residue was dissolved in Buffer A (S3, formic acid-soluble fraction). All fractions were analyzed using Western blotting with the anti-HtrA2/Omi anti-serum as described above.

RESULTS

Western Blot Analysis

In normal human brain homogenates, the anti-HtrA2/Omi anti-serum immunostained a single band at a molecular weight of approximately 36 kd (Fig. 1A). This corresponds to the molecular weight of the mature form of human HtrA2/Omi and indicates that the anti-serum recognizes HtrA2/Omi in human brain tissues. No specific immunopositive bands were detected in the membrane incubated with the preimmune serum (Fig. 1A). HtrA2/Omi immunoreactivity was detected in the S1 and S2 fractions from control and DLB brains, but the S3 fractions from both showed no HtrA2/Omi immunoreactivity on Western blot (Fig. 2).

HtrA2/Omi Immunoreactivities in Normal and Knockout Mice Brains

HtrA2/Omi immunoreactivity was observed in several types of neurons in the wild-type control mouse brain sections (Fig. 1B), but no specific immunopositive staining was found in the knockout mouse brain sections (Fig. 1C).

HtrA2/Omi Immunoreactivities in Normal and PD Brains

In the substantia nigra of control subjects, melanin-containing neurons generally showed mild to moderate HtrA2/Omi immunoreactivity (Fig. 3A). A similar

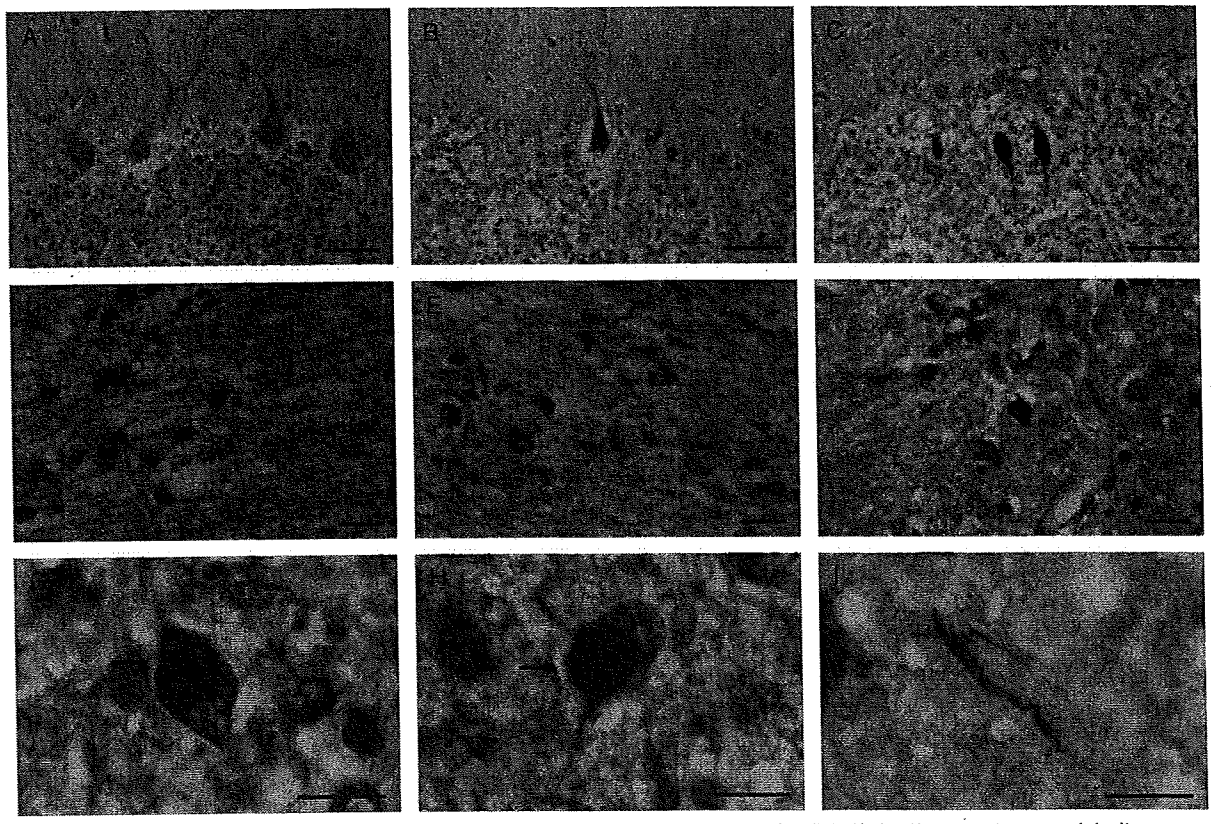

FIGURE 5. HtrA2/Omi immunoreactivity in normal **(A)** and multiple-system atrophy (MSA) **(B–I)** cases. Immunolabeling patterns of the Purkinje cells were similar in the control **(A)** and MSA cases **(B)**. Several torpedoes were also strongly immunopositive for HtrA2/Omi **(C)**. Numerous immunopositive glial cytoplasmic inclusions (GCIs) were found in the pontine nucleus **(D)**, cerebellar white matter **(E)**, and putamen **(F)**. In addition to the GCIs, neuronal cytoplasmic inclusions in the pontine base (**G** arrow, **H** arrow) and swollen neurites in the thalamus **(I)** were also immunoreactive for HtrA2/Omi. Cases illustrated: **A**: Control 1; **B, C, E**: MSA 3; **D, G, I**: MSA 2; **F**: MSA 6; **H**: MSA 7. Scale bars = **(A–C)** 50 μm; **(D–I)** 20 μm.

immunolabeling pattern was observed in the remaining neurons of the substantia nigra from patients with PD (Fig. 3B).

Classic LBs, which generally consist of an eosinophilic core plus a surrounding pale halo (Figs. 3C, E), had a ring-shaped HtrA2/Omi immunostaining pattern; dense accumulations of immunoreactive products were also found in the halos of these LBs (Figs. 3D, F). Some remaining neurons contained 2 or more HtrA2/Omi-immunopositive LBs (Fig. 3G). Pale bodies, which are well-defined, less eosinophilic structures (Fig. 3H), were also heterogeneously immunolabeled (Fig. 3I) and had abundant granular HtrA2/Omi immunoreactivity in their peripheries (Fig. 3I). HtrA2/Omi-immunopositive classic LBs were also found in neurons of the locus ceruleus, dorsal motor nucleus of the vagus, and nucleus basalis of Meynert (not shown).

HtrA2/Omi Immunoreactivities in Normal and DLB Brains

Neurons and glial cells, including oligodendrocytes, of the neocortices and hippocampus in normal controls showed mild to moderate HtrA2/Omi immunoreactivity, and some neurons had strong perinuclear immunoreactivity (Fig. 4A).

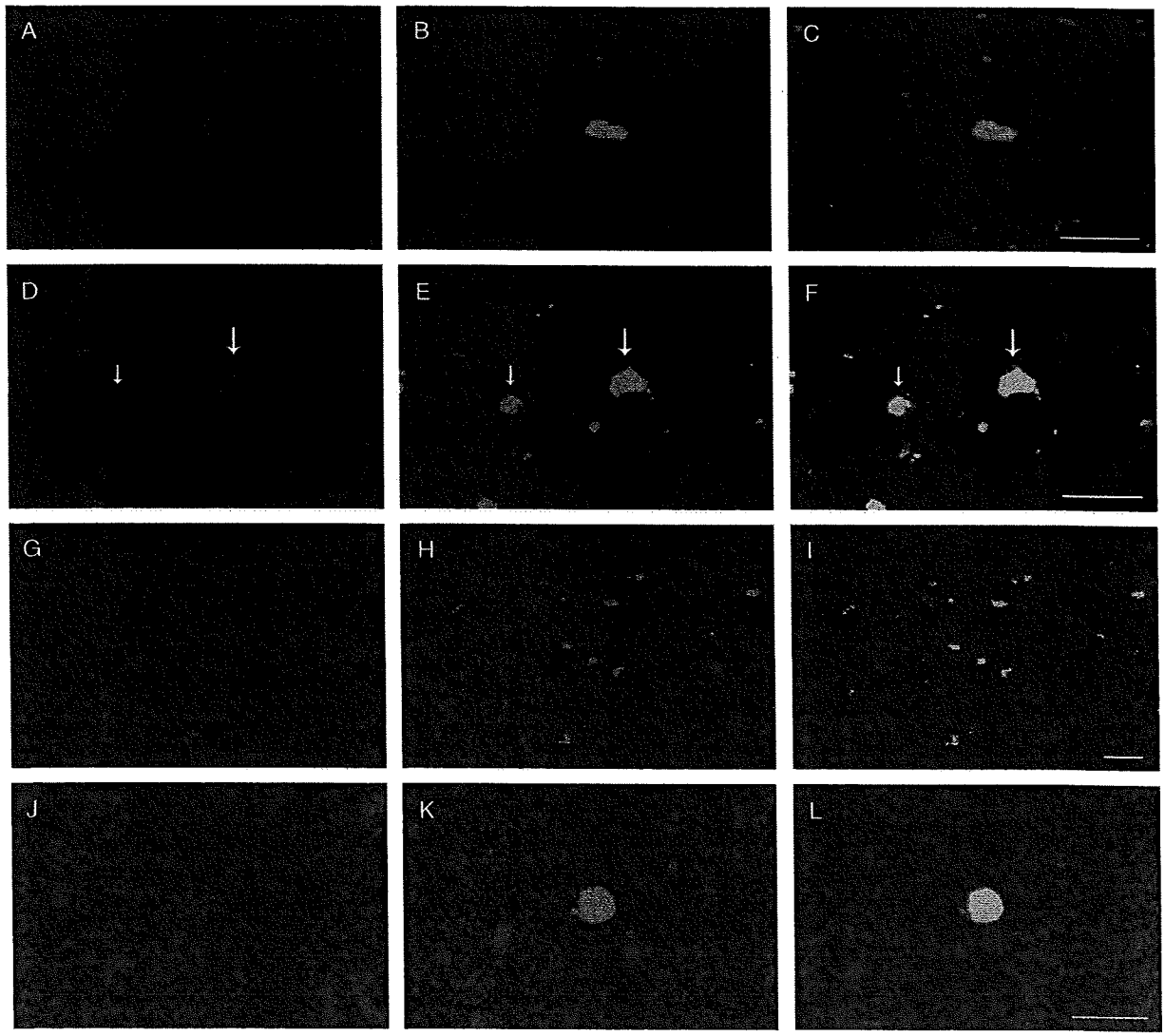

FIGURE 6. Double immunofluorescence staining for HtrA2/Omi **(A, D, G, J)** and α-synuclein **(B, E, H, K)** in the substantia nigra from a patient with Parkinson disease (PD) **(A–C**: PD 2**)**, cingulate gyrus from a patient with dementia with Lewy bodies (DLB) **(D–F**: DLB 4**)** and basis pontis from a patient with multiple system atrophy (MSA) **(G–L**: MSA 2**)**. The merged images showed that HtrA2/Omi and α-synuclein were colocalized in classic Lewy bodies (LBs) **(C)**, cortical LBs **(F)**, glial cytoplasmic inclusions **(I)** and neuronal cytoplasmic inclusions **(L)**. The large and small arrows in **D** to **F** indicate the same cortical LBs, respectively. Scale bars = (**C**, also for **A, B**; **F**, also for **D, E**; **I**, also for **G, H**; **L**, also for **J, K**) 20 μm.

TABLE 2. Summary of HtrA2/Omi-Immunopositive Inclusions

Type of Inclusions	No. Cases Analyzed	Anatomic Localization Evaluated	Average Percentage (%)*
Classic LBs	10 PD	Substantia nigra	68.9
Classic LBs	10 PD	Locus ceruleus	65.5
Classic LBs	10 PD	Dorsal motor nucleus of the vagus	54.9
Classic LBs	10 PD	Basal nucleus of Meynert	62.1
Cortical LBs	5 DLB	Superior frontal cortex	51.1
Cortical LBs	5 DLB	Cingulate cortex	55.8
Cortical LBs	5 DLB	Insular cortex	62.9
Cortical LBS	5 DLB	Parahippocampal cortex	65.7
GCIs	10 MSA	Internal capsule	78.2
GCIs	10 MSA	Putamen	76.9
GCIs	10 MSA	Middle cerebellar peduncle	86.3
GCIs	10 MSA	Cerebellar white matter	79.9

*See Materials and Methods.
LBs, Lewy bodies; GCIs, glial cytoplasmic inclusions; PD, Parkinson disease; DLB, dementia with Lewy bodies; MSA, multiple-system atrophy.

A similar immunolabeling pattern was observed in these regions in DLB patients, immunoreactivity was distributed densely throughout the somata of some remaining neurons (Fig. 4B). Only a few Lewy neurites were immunopositive for HtrA2/Omi (Fig. 4C).

Cortical LBs (i.e. ill-defined, eosinophilic inclusions without a conspicuous core and a clear halo [Figs. 4D, F, H]) were immunopositive for HtrA2/Omi (Figs. 4E, G, I). Some cortical LBs were immunostained diffusely (Fig. 4E), whereas others had partial immunostaining and strongly stained marginal zones (Fig. 4G) or central portions (Fig. 4I). These immunopositive cortical LBs were found throughout the cerebral cortical areas but were more numerous in cingulate, insular, and parahippocampal cortices. As in PD patients, the halos of classic LBs were intensely immunolabeled in DLB patients (not shown).

HtrA2/Omi Immunoreactivities in Normal and MSA Brains

Cerebellar Purkinje cells were mildly to moderately immunostained both in normal subjects (Fig. 5A) and in patients with MSA (Fig. 5B). The torpedoes, which were observed more often in the MSA cases, were also strongly immunopositive for HtrA2/Omi (Fig. 5C). Neuronal labeling patterns in substantia nigra, pontine nuclei, inferior olivary nucleus, and striatum in MSA patients were similar to those in the normal controls.

Glial cytoplasmic inclusions in the basis pontis (Fig. 5D), middle cerebellar peduncle, cerebellar white matter (Fig. 5E), putamen (Fig. 5F), and internal capsule were immunopositive in MSA patients. Strongly immunopositive neuronal cytoplasmic inclusions (NCIs) were found in some remaining neurons of the pons (Figs. 5G, H) and inferior olivary nucleus; a few dystrophic neurites were also densely immunopositive for HtrA2/Omi in various areas, including the basis pontis and thalamus (Fig. 5I). There were no significant differences in the immunolabeling patterns between the cases with MSA of cerebellar variant and of parkinsonian variant.

Double-Labeling Immunohistochemistry for HtrA2/Omi and α-Synuclein

Double-immunostained sections demonstrated HtrA2/Omi and α-synuclein colocalization in many classic LBs (Figs. 6A–C), cortical LBs (Figs. 6D–F), and GCIs (Figs. 6G–I). The colocalization of HtrA2/Omi and α-synuclein was also observed in some NCIs (Figs. 6J–L). Semiquantitative data on percentages of HtrA2/Omi-immunopositive LBs and GCIs are summarized in Table 2.

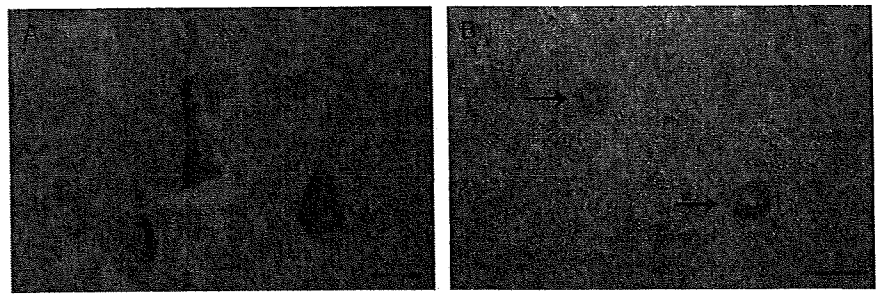

FIGURE 7. HtrA2/Omi immunoreactivity in the parahippocampal cortical areas from patients with Alzheimer disease (**A**: OD 2; **B**: OD 3). Some neurofibrillary tangles **(A)** and dystrophic neurites of senile plaques (**B**, arrows) are immunopositive for HtrA2/Omi. Scale bars = **(A, B)** 20 μm.

HtrA2/Omi Immunoreactivities in Brains With Other Diseases

HtrA2/Omi immunoreactivity was also observed in some neurofibrillary tangles (Fig. 7A) and dystrophic neurites of senile plaques (Fig. 7B) in the brains of patients with AD. By contrast, neuronal and glial inclusions in the case with frontotemporal dementia with parkinsonism linked to chromosome 17 and the case with frontotemporal lobar degeneration with ubiquitin-positive inclusions were immunonegative for HtrA2/Omi.

DISCUSSION

We demonstrate the widespread accumulation of HtrA2/Omi in α-synuclein-containing inclusions in the brains of patients with several types of α-synucleinopathies. To the best of our knowledge, this is the first detailed distribution of HtrA2/Omi immunoreactivity in the brains of these patients. In their study of mutations in the *HtrA2/Omi* gene, Strauss and colleagues (30) referred to the immunohistochemical localization of HtrA2/Omi in classic LBs. We also observed HtrA2/Omi immunoreactivity in the halos of classic LBs and demonstrated HtrA2/Omi immunoreactivity in cortical LBs and pale bodies in patients with PD and DLB, and in GCIs and NCIs in patients with MSA.

Both pale bodies and classic LBs are found in the pigmented neurons of the substantia nigra in patients with PD. Because pale bodies are generally considered to be precursors of classic LBs (9, 32), and both are immunopositive for α-synuclein (9, 12), the presence of HtrA2/Omi as well as of α-synuclein suggests that both may be involved in the formation of classic LBs in the early stages. The immunostaining of pale bodies was heterogeneous, but immunoreaction product was predominantly distributed at their margins. Because the halos of the classic LBs were densely immunopositive, these observations suggest that HtrA2/Omi may accumulate toward the marginal zones of the pale bodies and subsequently form the halos of classic LBs.

Cortical LBs were also immunopositive for HtrA2/Omi, but unlike classic LBs, most cortical LBs did not exhibit a ring-shaped labeling pattern. Some cortical LBs were immunostained diffusely, but HtrA2/Omi immunoreactivity was located mainly at their margins or central portions. Cortical LBs are usually poorly defined eosinophilic structures, and the central cores and peripheral halos usually observed in classic LBs are not evident (8, 9). These differences in structure may contribute to the different HtrA2/Omi-immunostaining patterns.

Since the discovery that 1-methyl-4-phenyl-1,2,3,6-tetrahydropyridine could cause PD-like symptoms in humans (33), several studies have shown that mitochondrial dysfunction plays an important role in the pathogenesis of PD (34). For example, the gene encoding PTEN-induced putative kinase 1 (PINK1) is responsible for PARK6-associated autosomal recessive juvenile parkinsonism (35), and PINK1 has been reported to be localized in the mitochondria (36, 37). Although the immunohistochemical localization of PINK1 in GCIs is controversial (37, 38), PINK1 immunoreactivity has also been found in LBs (37, 38). Recently, HtrA2/Omi was reported to be phosphorylated in a PINK1-dependent manner (39). Because in the present study, we demonstrate the mitochondria-related protein HtrA2/Omi in LBs, interactions between PINK1 and HtrA2/Omi may occur in LBs, and together they may be involved in LB formation.

Mitochondrial dysfunction can lead to apoptotic cell death. There is both neuronal apoptosis in the substantia nigra of patients with PD (40) and oligodendrocyte apoptosis in oligodendrocytes in the brains of patients with MSA (41). Some surviving dopaminergic neurons contain classic LBs in PD (8, 9), and many surviving oligodendrocytes harbor GCIs in MSA (14, 15). Whether these cytoplasmic inclusions induce apoptotic cell death or are protective of these cells from the toxic effects of misfolded proteins remains controversial, but several lines of evidence support the hypothesis that the formation of α-synuclein-containing inclusions may be cytoprotective (42, 43). In the present study, we found that both LBs and GCIs contained dense immunoreactivity for HtrA2/Omi, which in the cytosol might promote apoptosis. Based on these data, we suggest that these inclusions may trap HtrA2/Omi that has been released from the mitochondria and thus protect the dopaminergic neurons in PD and the oligodendrocytes in MSA from HtrA2/Omi-related apoptotic cell death.

A widespread distribution of GCIs in the central nervous system is the main pathologic feature of patients with MSA (14, 15, 44), and α-synuclein is a major component of GCIs (12, 16, 17), but the primary cause of MSA is still undetermined. The intense HtrA2/Omi immunoreactivity observed in GCIs as well as in NCIs and dystrophic neurites in the brains of patients with MSA in the present study suggests that HtrA2/Omi accumulates widely in MSA and that it may be one of the key proteins involved in MSA pathogenesis. Multiple-system atrophy is generally considered to be a sporadic disease, and although familial MSA cases have been identified (45), the genetic factors responsible for MSA remain unclear. Recently, null mutations in the *HtrA2/Omi* gene in mice were shown to lead to parkinsonism accompanied by striatal degeneration (29), a characteristic feature of MSA. Taken together, these results support the possibility that mutations of the gene encoding HtrA2/Omi could be involved in the pathogenesis of MSA. Further genetic analyses on HtrA2/Omi in patients with MSA are necessary.

In conclusion, we found that HtrA2/Omi immunoreactivity accumulated abundantly in brains with α-synucleinopathies, particularly in several types of inclusions containing insoluble α-synuclein, suggesting that HtrA2/Omi may be involved in the aggregation of α-synuclein. Several recent studies have shown that HtrA2/Omi plays an important role in the pathogenesis of AD by regulating β-amyloid precursor protein metabolism (46–48). We also observed the localization of HtrA2/Omi immunoreactivity in some inclusions in brains from patients with AD. These data suggest that HtrA2/Omi may be associated with the pathogenesis of a wide spectrum of neurodegenerative disorders, and further research on the interactions of HtrA2/Omi with α-synuclein will provide new insights into the pathologic mechanisms responsible for α-synucleinopathies.

ACKNOWLEDGMENT

The authors thank Hitomi Nakabayashi for her excellent technical assistance.

REFERENCES

1. Polymeropoulos MH, Lavedan C, Leroy E, et al. Mutation in the α-synuclein gene identified in families with Parkinson's disease. Science 1997;276:2045–47
2. Krüger R, Kuhn W, Müller T, et al. Ala30Pro mutation in the gene encoding α-synuclein in Parkinson's disease. Nat Genet 1998;18: 106–8
3. Zarranz JJ, Alegre J, Gómez-Esteban JC, et al. The new mutation, E46K, of α-synuclein causes Parkinson and Lewy body dementia. Ann Neurol 2004;55:164–73
4. Singleton AB, Farrer M, Johnson J, et al. α-Synuclein locus triplication causes Parkinson's disease. Science 2003;302:841
5. Chartier-Harlin M-C, Kachergus J, Roumier C, et al. α-Synuclein locus duplication as a cause of familial Parkinson's disease. Lancet 2004;364: 1167–69
6. Ibáñez P, Bonnet A-M, Débarges B, et al. Causal relation between α-synuclein gene duplication and familial Parkinson's disease. Lancet 2004;364:1169–71
7. Forno LS, Norville RL. Ultrastructure of Lewy bodies in the stellate ganglion. Acta Neuropathol 1976;34:183–97
8. Pollanen MS, Dickson DW, Bergeron C. Pathology and biology of the Lewy body. J Neuropathol Exp Neurol 1993;52:183–91
9. Takahashi H, Wakabayashi K. The cellular pathology of Parkinson's disease. Neuropathology 2001;21:315–22
10. Spillantini MG, Schmidt ML, Lee VM-Y, et al. α-Synuclein in Lewy bodies. Nature 1997;388:839–40
11. Wakabayashi K, Matsumoto K, Takayama K, et al. NACP, a presynaptic protein, immunoreactivity in Lewy bodies in Parkinson's disease. Neurosci Lett 1997;239:45–48
12. Wakabayashi K, Hayashi S, Kakita A, et al. Accumulation of α-synuclein/NACP is a cytopathological feature common to Lewy body disease and multiple system atrophy. Acta Neuropathol 1998;96: 445–52
13. Graham JG, Oppenheimer DR. Orthostatic hypotension and nicotine sensitivity in a case of multiple system atrophy. J Neurol Neurosurg Psychiatry 1969;32:28–34
14. Papp MI, Kahn JE, Lantos PL. Glial cytoplasmic inclusions in the CNS of patients with multiple system atrophy (striatonigral degeneration, olivopontocerebellar atrophy and Shy-Drager syndrome). J Neurol Sci 1989;94:79–100
15. Nakazato Y, Yamazaki H, Hirato J, et al. Oligodendroglial microtubular tangles in olivopontocerebellar atrophy. J Neuropathol Exp Neurol 1990; 49:521–30
16. Gai WP, Power JHT, Blumbergs PC, et al. Multiple-system atrophy: A new α-synuclein disease? Lancet 1998;352:547–48
17. Wakabayashi K, Yoshimoto M, Tsuji S, et al. α-Synuclein immunoreactivity in glial cytoplasmic inclusions in multiple system atrophy. Neurosci Lett 1998;249:180–82
18. Spillantini MG, Goedert M. The α-synucleinopathies: Parkinson's disease, dementia with Lewy bodies, and multiple system atrophy. Ann N Y Acad Sci 2000;920:16–27
19. Deveraux QL, Takahashi R, Salvesen GS, et al. X-linked IAP is a direct inhibitor of cell-death proteases. Nature 1997;388:300–4
20. Takahashi R, Deveraux Q, Tamm I, et al. A single BIR domain of XIAP sufficient for inhibiting caspases. J Biol Chem 1998;273:7787–90
21. Deveraux QL, Reed JC. IAP family proteins—suppressors of apoptosis. Genes Dev 1999;13:239–52
22. Suzuki Y, Imai Y, Nakayama H, et al. A serine protease, HtrA2, is released from the mitochondria and interacts with XIAP, inducing cell death. Mol Cell 2001;8:613–21
23. Hegde R, Srinivasula SM, Zhang Z, et al. Identification of Omi/HtrA2 as a mitochondrial apoptotic serine protease that disrupts inhibitor of apoptosis protein-caspase interaction. J Biol Chem 2002;277:432–38
24. Martins LM, Iaccarino I, Tenev T, et al. The serine protease Omi/HtrA2 regulates apoptosis by binding XIAP through a Reaper-like motif. J Biol Chem 2002;277:439–44
25. Verhagen AM, Silke J, Ekert PG, et al. HtrA2 promotes cell death through its serine protease activity and its ability to antagonize inhibitor of apoptosis proteins. J Biol Chem 2002;277:445–54
26. Srinivasula SM, Gupta S, Datta P, et al. Inhibitor of apoptosis proteins are substrates for the mitochondrial serine protease Omi/HtrA2. J Biol Chem 2003;278:31469–72
27. Yang Q-H, Church-Hajduk R, Ren J, et al. Omi/HtrA2 catalytic cleavage of inhibitor of apoptosis (IAP) irreversibly inactivates IAPs and facilitates caspase activity in apoptosis. Genes Dev 2003;17:1487–96
28. Suzuki Y, Takahashi-Niki K, Akagi T, et al. Mitochondrial protease Omi/HtrA2 enhances caspase activation through multiple pathways. Cell Death Differ 2004;11:208–16
29. Martins LM, Morrison A, Klupsch K, et al. Neuroprotective role of the Reaper-related serine protease HtrA2/Omi revealed by targeted deletion in mice. Mol Cell Biol 2004;24:9848–62
30. Strauss KM, Martins LM, Plun-Favreau H, et al. Loss of function mutations in the gene encoding Omi/HtrA2 in Parkinson's disease. Hum Mol Genet 2005;14:2099–111
31. Mckeith IG, Dickson DW, Lowe J, et al. Diagnosis and management of dementia with Lewy bodies: Third report of the DLB Consortium. Neurology 2005;65:1863–72
32. Dale GE, Probst A, Luthert P, et al. Relationships between Lewy bodies and pale bodies in Parkinson's disease. Acta Neuropathol 1992;83:525–29
33. Langston JW, Ballard P, Tetrud JW, et al. Chronic Parkinsonism in humans due to a product of meperidine-analog synthesis. Science 1983; 219:979–80
34. Fukae J, Mizuno Y, Hattori N. Mitochondrial dysfunction in Parkinson's disease. Mitochondrion 2007;7:58–62
35. Valente EM, Abou-Sleiman PM, Caputo V, et al. Hereditary early-onset Parkinson's disease caused by mutations in PINK1. Science 2004;304: 1158–60
36. Silvestri L, Caputo V, Bellacchio E, et al. Mitochondrial import and enzymatic activity of PINK1 mutants associated to recessive parkinsonism. Hum Mol Genet 2005;14:3477–92
37. Gandhi S, Muqit MMK, Stanyer L, et al. PINK1 protein in normal human brain and Parkinson's disease. Brain 2006;129:1720–31
38. Murakami T, Moriwaki Y, Kawarabayashi T, et al. PINK1, a gene product of PARK6, accumulates in a-synucleinopathy brains. J Neurol Neurosurg Psychiatry 2007;78:653–55
39. Plun-Favreau H, Klupsch K, Moisoi N, et al. The mitochondrial protease HtrA2 is regulated by Parkinson's disease-associated kinase PINK1. Nat Cell Biol 2007;9:1243–52
40. Mochizuki H, Goto K, Mori H, et al. Histochemical detection of apoptosis in Parkinson's disease. J Neurol Sci 1996;137:120–23
41. Probst-Cousin S, Rickert CH, Schmid KW, et al. Cell death mechanisms in multiple system atrophy. J Neuropathol Exp Neurol 1998;57:814–21
42. Tanaka M, Kim YM, Lee G, et al. Aggresomes formed by α-synuclein and synphilin-1 are cytoprotective. J Biol Chem 2004;279:4625–31
43. Sawada H, Kohno R, Kihara T, et al. Proteasome mediates dopaminergic neuronal degeneration, and its inhibition causes α-synuclein inclusions. J Biol Chem 2004;279:10710–19
44. Papp MI, Lantos PL. The distribution of oligodendroglial inclusions in multiple system atrophy and its relevance to clinical symptomatology. Brain 1994;117:235–43
45. Soma H, Yabe I, Takei A, et al. Heredity in multiple system atrophy. J Neurol Sci 2006;240:107–10
46. Park H-J, Seong Y-M, Choi J-Y, et al. Alzheimer's disease-associated amyloid beta interacts with the human serine protease HtrA2/Omi. Neurosci Lett 2004;357:63–67
47. Park H-J, Kim S-S, Seong Y-M, et al. β-Amyloid precursor protein is a direct cleavage target of HtrA2 serine protease: Implications for the physiological function of HtrA2 in the mitochondria. J Biol Chem 2006; 281:34277–87
48. Huttunen HJ, Guénette SY, Peach C, et al. HtrA2 regulates β-amyloid precursor protein (APP) metabolism through endoplasmic reticulum-associated degradation. J Biol Chem 2007;282:28285–95

ファルマシア

別刷

社団法人
日本薬学会
The Pharmaceutical Society of Japan

SEMINAR セミナー

筋萎縮性側索硬化症(ALS)の治療戦略

村上　学
Gaku MURAKAMI
京都大学大学院医学研究科
臨床神経学大学院生

井上治久
Haruhisa INOUE
京都大学物質-細胞統合システム拠点
iPS 細胞研究センター准教授

高橋良輔
Ryosuke TAKAHASHI
京都大学大学院医学研究科
臨床神経学教授

1 はじめに

神経変性疾患は，特定の神経系が選択的に変性・細胞死を生じる疾患の総称である．神経変性疾患の神経病理学的な特徴は，神経細胞及び非神経細胞の内外に認められる脳内のタンパク質凝集物(封入体)である．そのうち筋萎縮性側索硬化症(ALS)は，上位及び下位運動ニューロンが選択的に変性していく疾患である．40～70歳代で発症し，平均発症年齢は約65歳である．通常発症後四肢及び球麻痺が進行性の経過をたどり，3～5年で呼吸不全などで死亡することが多い．ALSの約90%は孤発性，約10%は家族性である.[1] 高次脳機能など，その他の神経系には目立った症状を認めず，運動神経が選択的に侵され，患者の苦痛が大きいこと，症状の重篤さにも関わらず有効な治療がないことより，治療方法の開発が精力的に行われてきた．

1993年に，家族性ALSの一部はCu/Zn superoxide dismutase(SOD 1)の変異による[1]ことが発見された．その後の研究で，家族性ALSの約20%がSOD 1変異によるとされたが，最近の学会報告では日本では家族性ALSの50%前後がSOD 1変異による．また，孤発性ALSの数%がSOD 1変異によることも明らかになった.[2] 変異SOD 1は活性を残存しているものもあり，その活性低下と臨床経過とは相関せず，変異SOD 1タンパク質の毒性による運動神経変性と考えられる．

さらに最近になって，ALS患者剖検脳脊髄運動神経細胞のタンパク質凝集物の主要構成成分がtransactivation responsive element(TAR) DNA-binding protein of 43 kDa(TDP-43)であることが判明した.[3,4] 驚くべきことに，その後の遺伝学的解析によって，家族性及びごく一部の一見孤発性にみえるALSが，TDP-43遺伝子の変異によって発症することも次々と報告された.[5]

本稿では，SOD 1及びTDP-43の関与するALSの治療戦略について概説する．

2 ALSの病態仮説

SOD 1関連ALS

ALSの病態モデルとして，変異SOD 1トランスジェニックマウスによる研究が精力的に行われ，様々な病態仮説が提唱されている．酸化ストレス，グルタミン酸による興奮毒性，炎症性機序，ミトコンドリア異常，軸索輸送障害，小胞体ストレス，ユビキチン・プロテアソームシステムやオートファジーなどのタンパク質品質管理機構の破綻，凝集タンパク質による細胞毒性などである．

また変異SOD 1トランスジェニックマウスモデルの解析により，変異SOD 1が神経細胞に対して毒性を発揮するだけでなく(自律性神経細胞毒性)，アストロサイトやミクログリアといった非ニューロン細胞内の変異SOD 1タンパク質発現が，ニューロンの変性を促進するという，非自律性神経細胞毒性機序も報告されている.[6,7]

しかし変異SOD 1患者及びモデルマウスでは，一部報告[8]を除いて細胞内TDP-43タンパク質凝集がみられず，核移行性の変化も原則的にはみられない[9]ため，孤発性ALSのモデルとしては問題点が指摘されている．

TDP-43関連ALS

近年発表されたTDP-43の病態仮説については，さらに他の機序が提唱されている．ALS患者剖検組織においてはTDP-43のリン酸化,[3,10] カスパーゼによる切断[11]がみられ，TDP-43に対する免疫組織染色では核の染色性が失われ細胞質に移行する.[3,4] TDP-43はRNA結合ドメインを持ち，種々のRNA及びタンパク質に結合して，核内において

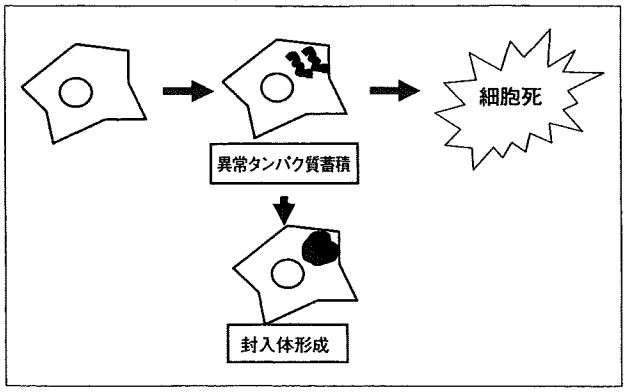

図1 異常タンパク質による細胞毒性

異常タンパク質が蓄積すると，それを分解するだけでなく，封入体に凝集して無毒化する．しかし，細胞の処理能力を超えるタンパク質が蓄積すると，細胞死を引き起こす．

mRNAのスプライシングなどを行っている.[12] そのため，細胞内の修飾されたTDP-43の核移行が低下することにより核内のTDP-43の機能低下を来たし，毒性を発揮するという機能喪失モデルも提唱されている．

他の神経変性疾患同様，変異タンパク質が毒性を獲得して神経細胞障害，細胞死を起こす可能性も考えられる(gain of toxic functionモデル)(図1)．細胞内では，異常タンパク質を分解したり，無毒な封入体に凝集させることで対応していくと考えられるが，その防御機構を超えて異常タンパク質が蓄積すると細胞毒性を発揮して細胞死を引き起こすものと考えられる．

3 ALS治療開発の現状

先述のように，ALSでは変異SOD1トランスジェニックマウスが家族性ALSの病態モデルとして確立しており，その動物モデルによる治療法開発が行われている．例えば，酸化ストレスに対し抗酸化剤であるビタミンEや，ミトコンドリア機能改善目的にコエンザイムQ_{10}で運動神経症状の進行を遅延し生存期間を延長し，有効性が認められた.[13] また，シクロオキシゲナーゼを抑制し抗炎症作用を有するミノサイクリンなども有効性が認められた.[13]

また，アストロサイトのグルタミン酸トランスポーター1の発現を上昇させる既存薬剤のハイスループット・スクリーニングを行い，第3世代セフェム系抗生物質であるセフトリアキソンが発見され,[14] ヒトへの臨床試験も行われている．

他に，神経栄養因子による神経保護を目指した治療も検討されている．インスリン様増殖因子(IGF-1)などが有効性を認めた.[13]

そのほか様々な治療アプローチがなされてきたが，いずれの薬剤も臨床試験で明らかな有効性を証明できず，現在ALSに対し有効性が証明された薬剤はグルタミン酸遊離阻害や興奮性アミノ酸受容体との非競合的阻害，電位依存性Na^+チャネル阻害等の作用を有するリルゾールのみである．しかしリルゾールによる延命効果は約3か月に留まり，筋力・運動機能の改善は望めず，その効果は限定的である.[15]

4 SOD 1タンパク質量制御による家族性ALSの治療法

変異SOD1トランスジェニックマウスでは，トランスジーンのコピー数が多いほど表現型が重篤である.[16] また，変異SOD1トランスジェニックラットでは，トランスジーンのコピー数の多いラットのみがALSを発症し，コピー数の少ないラットでは発症しない.[17] したがって，変異SOD1に関連したALSでは，変異SOD1の量を減らすことが治療につながる可能性がある．

実際の実験治療として，RNA干渉やantisense oligonucleotideを用いてタンパク質発現量を低下させることで病態を改善した，という報告がある．RNA干渉を用いた実験[18]では，変異SOD1 mRNAに相補的なsiRNAを変異SOD1マウスにかけ合わせたダブルトランスジェニックマウスで，その生存期間が著明に延長したという報告がある．また，antisense oligonucleotideを脳室内に投与し，変異SOD1タンパク質の細胞内産生抑制を行ったマウスでも表現型の改善が見られる.[19]

さらに，lox配列で変異*SOD1*遺伝子を挟みSOD1本来のプロモーターで変異SOD1を発現して，通常の変異SOD1マウスと同様にALSを発症するトランスジェニックマウスを組織特異的Cre

発現マウスとかけ合わせることによって，運動ニューロンでのみ変異SOD1発現を低下させるとALSの発症が遅延し，ミクログリアでのみ変異SOD1発現を低下させると疾患の進行を遅らせたという報告がある.[6] 同様の手法で，アストロサイト内変異SOD1発現低下により疾患の進行を遅らせたという報告もある.[7]

他の神経変性疾患モデルでも，原因タンパク質発現量を減少させることで治療につながる可能性が示唆されている．ハンチントン病はハンチンチン(Htt)というタンパク質のポリグルタミン(polyQ)が異常に増えることで，そのタンパク質の凝集，神経細胞変性が認められる疾患であり，polyQ Httを過剰発現するトランスジェニックマウスはハンチントン病のモデルとして知られている．そのマウスのpolyQ発現量を，Tet-Offシステムを用いて後天的に減少させると，発症を抑えられたという報告がある.[20] また，アルツハイマー病モデルである変異タウトランスジェニックマウスでも，同様のシステムで発現量を抑えることで，記憶機能の改善及び神経細胞変性の抑制が観察されている.[21]

以上から，我々はSOD1の転写を抑制してSOD1タンパク質量を減少する低分子を，低分子化合物・既存薬ライブラリのハイスループット・スクリーニング・システム(図2)を構築して，家族性ALS治療薬スクリーニングを行っている．我々はSOD1の本来のプロモーターの支配下にレポーター遺伝子としてルシフェラーゼを発現するコンストラクトを構築した．

化合物がプロモーターに作用し転写を抑制すれば，ルシフェラーゼの発現量が低下しルシフェラーゼの基質から産生される蛍光物質の量が低下する．アストロサイトが非自律性神経細胞死，疾患の進行に関連することから，ヒトアストロサイト由来の細胞株を使用している．また，ルシフェラーゼ反応基質を96-ウェル・プレート上で自動分注後吸光度を測定する装置を用いて測定している．このような方法でこれまでに9,600種類の化合物をスクリーニングし，蛍光物質の産生を減少させる，すなわちSOD1の転写を抑制する化合物を177種類見いだしており，これからさらにALSモデル細胞やALSモデル動物での効果を確認して，臨床的に有用な化合物を絞り込んでいく予定である．低分子化合物は，大量生産が可能であり，安価で安定した供給を行うことが可能となる．また，既存薬を用いればヒトへの使用における安全性も既に確認されており，速やかな臨床への応用も可能となる．我々の開発した方法は，ALS治療開発における新たなアプローチの1つとなるものと考える．

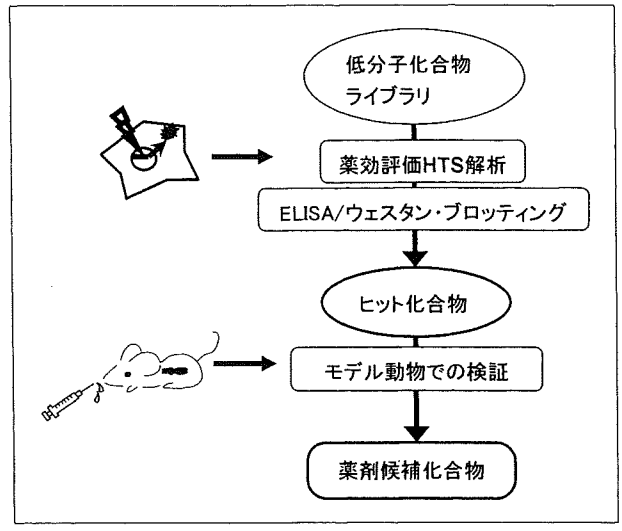

図2 我々のALS治療開発戦略の概要

SOD1プロモータ下にルシフェラーゼを発現するコンストラクトを導入した，ヒトアストロサイト由来細胞株を用いて，SOD1転写を抑制する化合物をスクリーニングする．ELISAやウェスタン・ブロッティングでSOD1タンパク質量を特異的に減少する化合物を抽出する．変異SOD1トランスジェニックマウスでその効果を確認する．

5 SOD1タンパク質を減少させることによる問題点

SOD1は細胞内に発生したsuperoxide radicalsを過酸化水素に分解する酵素であり，抗酸化ストレス酵素の1つに挙げられる．したがって，SOD1を減少させることは，酸化ストレス反応に対する脆弱性を来たす可能性がある．

SOD1ノックアウトマウスの解析によると，脊髄運動神経軸索を切断した後の神経細胞死がSOD1非ノックアウトマウスに比して多く見られる.[22] ほかに，神経筋接合部の形成不全や軸索変性が，高齢のSOD1ノックアウトマウスで見られるという報告もある.[23] したがって，SOD1を大きく低下させることは脊髄運動神経変性を来たす可能性

がある．

ただし，SOD 1 ノックアウトマウスの寿命は非ノックアウトマウスに比べ著変が見られない．[24] さらに，SOD 1 ヘテロノックアウトマウスはノックアウトマウスに比して軸索切断による神経細胞死の程度が軽度である．[24] また，他のアンチオキシダントによる代償も期待できるため，SOD 1 を特異的部分的に減少させることが，重篤な副作用を来たさずに，治療効果を得るために重要である．

さらに，コピー数が多い野生型 *SOD1* 遺伝子のトランスジェニックマウスでも軸索変性やミトコンドリアの変性，脊髄運動ニューロンの減少が，高齢になれば出現することが報告されている．[24] 変異型 SOD 1 と野生型 SOD 1 のダブルトランスジェニックマウスは，野生型 SOD 1 量に応じて進行が速くなるとの報告[24]もあり，野生型 SOD 1 細胞内産生も制御する試みは相乗的に有効である可能性がある．

先述のように，他のアプローチで明らかな有効性を認めた治療がほとんどないこともあり，原因となる異常タンパク質を直接減少させるアプローチが有望と考えられることから，SOD 1 タンパク質量を減少させる有用性は，部分的特異的に行うことができれば，そのリスクよりも大きく，根本的な治療につながると考えられる．

6 孤発性 ALS に対する治療的アプローチ

先述のように，孤発性 ALS では TDP-43 タンパクの細胞質内封入体を認め，核における染色性が失われている．核移行シグナルを欠損させた *TDP-43* 遺伝子ないし，易凝集性の高い C 末端 *TDP-43* 遺伝子に GFP を付して導入した TDP-43 凝集細胞モデルを用いて，タンパク質凝集を抑制させる薬剤が報告されている．[25]

ただし，TDP-43 に関連した ALS の病態生理はまだ未解明の部分が多く，今後 TDP-43 の生理的機能及び変異 TDP-43 の神経細胞に対する影響の詳細な解析がまたれる．

7 おわりに

ALS，特に変異 SOD 1 関連 ALS の病態に沿った治療戦略について概説した．精力的な研究がなされてはいるが，未だ病勢を決定的に改善する薬剤は開発されていない．この難病に対する治療法が早く発見され，多くの患者が治療される日が来ることを望む．

文　献

1) Rosen D. R. *et al*., *Nature*, 362, 59-62 (1993).
2) Andersen P. M. *et al*., *Curr. Neurol. Neurosci. Rep*., 6, 37-46 (2006).
3) Arai T. *et al*., *Biochem. Biophys. Res. Commun*., 351, 602-611 (2006).
4) Neumann M. *et al*., *Science*, 314, 130-133 (2006).
5) Lagier-Tourenne C. *et al*., *Cell*, 136, 1001-1004 (2009).
6) Boilee S. *et al*., *Science*, 312, 1389-1392 (2006).
7) Yamanaka K. *et al*., *Nat. Neurosci*., 11, 251-253 (2008).
8) Shan X. *et al*., *Neurosci. Lett*., 458, 70-74 (2009).
9) Mackenzie I. *et al*., *Ann. Neurol*., 61, 427-434 (2007).
10) Hasegawa M. *et al*., *Ann. Neurol*., 64, 60-70 (2008).
11) Zhang Y. J. *et al*., *J. Neurosci*., 27, 10530-10534 (2007).
12) Buratti E. *et al*., *Front. Biosci*., 13, 867-878 (2008).
13) Brujin L. *et al*., *Expert. Rev. Neurother*., 6, 417-428 (2006).
14) Rothstein J. D. *et al*., *Nature*, 433, 73-77 (2005).
15) Miller R. G. *et al*., *Cochrane Database Syst Rev*., (1), CD 001447 (2007).
16) Dal Canto M. *et al*., *Brain Res*., 676, 25-40 (1995).
17) Nagai M. *et al*., *J. Neurosci*., 21, 9246-9254 (2001).
18) Saito Y. *et al*., *J. Biol. Chem*., 280, 42826-42830 (2005).
19) Smith R. A. *et al*., *J. Clin. Invest*., 116, 2290-2296 (2006).
20) Yamamoto A. *et al*., *Cell*, 101, 57-66 (2000).
21) SantaCruz K. *et al*., *Science*, 309, 476-481 (2006).
22) Reasume A. *et al*., *Nat. Genet*., 13, 43-47 (1996).
23) Flood D. G. *et al*., *Am. J. Pathol*., 155, 663-672 (1999).
24) Jaarsma D. *et al*., *Neurobiol. Dis*., 7, 623-643 (2000).
25) Yamashita M. *et al*., *FEBS Lett*., 583, 2419-2424 (2009).

を計算する。浸透圧ギャップは血漿浸透圧実測値と計算値（上記の間で提示された式より計算）との差で、通常10 mOsm/kgH_2O以下である。これが10 mOsm/kgH_2O以上を示す場合には、マンニトール、エタノール、メタノール、エチレングリコール、トルエンなど、外因性浸透圧物質の増加が考えられる。

たん漿膠質浸透圧

再び収的巨大な粒子であるコロイる。子が懸濁液を形成しているようロモ状態でも、浸透圧を形成する。

ゾ浸透圧を膠質浸透圧（colloid osmotic pressureまたはoncotic pressure）と呼ぶ。膠質浸透圧は、一定容積中に含まれるコロイド粒子の数が多いほど大きくなる。血漿浸透圧と異なり、氷点降下法では測定できない。臨床的には、血漿蛋白質の約6割を占めるアルブミン1g／dℓにつき5・5 mmHg、4・5g／dℓで約25 mmHgの膠質浸透圧を示す。これは血漿全膠質浸透圧の8～9割に相当し、間質から血管に向かう力である。

ネフローゼ症候群や肝硬変のように血漿アルブミン濃度が減少する病態では、血漿膠質浸透圧が低下し血管内から間質に水の移動が生じ、浮腫が出現することになる。

文　献
1）武藤重明：日医雑誌135：S198，2006.

◆◆◆回　答◆◆◆
自治医科大学透析部／腎臓内科教授　武藤重明
京都大学臨床神経学（神経内科）・高橋良輔教授に。
（熊本県　N）

パーキンソン病の神経細胞移植治療

Q 神経細胞を移植したパーキンソン病患者の場合、健康なはずの移植された細胞にパーキンソン病の病理所見が出現することが報告された（Nature Medicine, 2008）。以下について。

(1)移植手術はパーキンソン病の根本治療法となりうるのか。

(2)近年、神経新生（neurogenesis）の研究が盛んであるが、この研究はパーキンソン病の新しい治療ターゲットとして有望なのか。

A Nature Medicineの5月号に掲載されたスウェーデンとアメリカとカナダの3グループからの論文に基づいたご質問である[1)-3)]。パーキンソン病の病理を特徴づけるのは、α-シヌクレインの凝集であるレビー小体である。上記3論文の結果をまとめると、胎児の黒質ドーパミン神経細胞を移植されて4～16年を経た計8例のパーキンソン病患者剖検例を調べたところ、驚くべきことに移植後10年以上を経た3例で移植片中の本来は健康なドーパミン神経にレビー小体が形成されていることが見出された。これはレビー小体病理がパーキンソン病患者組織から移植片に〝伝播〟するという、これまで神経変性疾患ではプリオン病でしか知られていなかったメカニズムが、パーキンソン病でも働くことを示したことになる。

〝伝播〟が生じるメカニズムに関してはまだ分からないが、移植後10年以内の5例の移植片ではレビー小体形成は見られなかったことから、少なくとも〝伝播〟には10年は必要なことが推察される。また、1例では移植後14年を経ていても移植片にレビー小体形成が見られていない。この例とレビー小体ができた例との違いの一つは、前者ではミクログリアの活性化が乏しかったことで、レビー小体〝伝播〟への炎症の関与をうかがわせる。

その他、酸化的ストレス、興奮毒性、神経栄養因子の欠乏などがメカニズムとして提唱されており、今後その解明はパーキンソン病の病態解明の上できわめて重要な課題となるであろう[4)]。

ただ、気をつけなければならないのは、レビー小体の形成が細胞の機能や生存に与える影響がまったく不明なことである。レビー小体は、それ自体が異常構造として細胞毒性を持つという考えから、レビー小体は毒性を持つ異常蛋白質を封じ込めるために作られるものであり、細胞保護的に働いてい

るというものまで様々な説があり、決着がついていない。移植片にレビー小体ができるからといって、その細胞が障害されるとは限らないのである。

また、移植後10年以上を経ないとレビー小体形成は見られないことから、たとえレビー小体に毒性があったとしても10年以内の効果は十分望みうることになる。胎児黒質移植自体は2件の二重盲検試験で有意な症状の改善効果がなく、異な不随意運動が生じるなどの副作用があることが示され、現在中われていないが、広く移植治療の一つものは方法論の改善で有用段階療法になる可能性は秘めておそのような意味で、今後も新1)な治療の選択肢として研究を続けるべきと思われる。

神経新生の治療に関しても同様の理由で、Nature Medicineの論文の結果が、治療法そのものを否定することにはならない。動物実験ではあるが、海馬における神経新生が抗うつ薬の効果発現に必須であることが示された[5]。これは、神経新生治療がパーキンソン病を含めた様々な神経疾患でも有用であることを強く示唆している。

パーキンソン病でも黒質ドーパミン神経の新生を示唆する報告があり、期待が持たれる[6]。ただし、一方でレビー小体が移植細胞、新生した細胞に生じた場合、それが細胞機能に与える影響を正確に評価する研究も進め、移植治療、神経新生治療の可能性と限界を明らかにすることが、これらの治療を将来的に現実のものとする上で重要であろう。

文献

1) Li JY, et al : Nature Med 14 : 501, 2008.
2) Kordower JH, et al : Nature Med 14 : 504, 2008.
3) Mendez I, et al : Nature Med 14 : 507, 2008.
4) Brundin P, et al : Nat Rev Neurosci 9 : 741, 2008.
5) Santarelli L, et al : Science 301 : 805, 2003.
6) Yoshimi K, et al : Ann Neurol 58 : 31, 2005.

◆◆◆回　答◆◆◆

京都大学医学研究科臨床神経学（神経内科）教授

高橋良輔

赤痢アメーバ症の診断と治療

Q 赤痢アメーバ症の診断と治療について、以下を。

(1)糞便検体の採取方法（顕微鏡検査用、培養検査用）。

(2)血液検査用の検体採取方法（検査名、検査結果の判読）。

(3)治療方法、治療期間。

(4)治療効果の確認方法。

（東京都　M）

A 糞便の顕微鏡検査で赤痢アメーバの嚢子あるいは栄養型に一致する形態を確認しても、赤痢アメーバ（*Entamoeba histolytica*）と報告してはならない。赤痢アメーバないしは非病原性のアメーバ（*E.histolytica*/*E.dispar*, 以下Eh/Edと略）と報告すべきである。赤痢アメーバ症を疑わせる症状がある場合、Eh/Edの検出をもって治療適応となる。健康人から検出されたEh/Edは治療適応とならない[1]。

(1)結果報告書に赤痢アメーバと記述できるのは、赤痢アメーバに特異的な検査を実施した場合のみである。赤痢アメーバの検査は国立感染症研究所あるいは地方衛生研究所で実施可能である[2]。検体採取法はそちらの指示に従っていただきたい。

自らの手で確認したい場合は、赤痢アメーバ抗原検出キットであるE. HISTOLYTICA II（関東科学から購入可）を入手すればよい。ただし、これは正式な検査法として認められていない。このため、法律上「診断に用いてはならない」ことになっている。

(2)アメーバ性肝膿瘍では、必ずしも糞便中に赤痢アメーバが検出できるとは限らない。血中抗赤痢アメーバ抗体の検出をもって、抗アメーバ薬の適否を判断する場合が多い。詳細は、参考文献をご覧いただきたい[2]。

(3)治療方法

第1選択薬はメトロニダゾールの経口投与である。海外の文献では2250mg/日の記述もみられるが、日本人には、1500mg分3、10日間で十分である[3]。なお、

Experimental Neurology 217 (2009) 235–236

Contents lists available at ScienceDirect

Experimental Neurology

journal homepage: www.elsevier.com/locate/yexnr

Commentary

Edaravone in ALS

Ryosuke Takahashi*

Department of Neurology, Kyoto University Graduate School of Medicine, 54 Shogoin-Kawaharacho, Sakyoku, Kyoto 606-8507, Japan

ARTICLE INFO

Article history:
Received 30 December 2008
Revised 28 February 2009
Accepted 3 March 2009
Available online 10 March 2009

Amyotrophic lateral sclerosis (ALS) is a devastating neurodegenerative disorder characterized by progressive and relatively selective degeneration of upper and lower motor neurons. Patients suffer from atrophy and paralysis of systemic voluntary muscles including respiratory muscles, leading to respiratory failure and subsequent death 3–5 years after the disease onset. Effective therapy for ALS that ameliorates its clinical course is still not known (Mitchell and Borasio, 2007).

Although ALS usually develops sporadically, 5 to 10% of cases are familial and hereditary. Twenty percent of familial ALS (FALS) are caused by mutations in the *copper and zinc-dependent superoxide dismutase* (*SOD1*) gene, which was first reported in 1993 (Rosen et al., 1993). Mutant SOD1 brought a breakthrough to this field, since mutant SOD1 transgenic mice recapitulate the clinical symptoms and pathological findings of human FALS (Gurney et al., 1994). Mutant SOD1 transgenic mouse models provided invaluable tools for testing effective drugs which extend their lifespan. Up to now, more than 20 drugs have been claimed to be effective in the therapy of mouse ALS.

A big problem, however, is arising: none of these drugs have yet to be shown to be effective as well in human sporadic ALS (SALS) patients (Benatar, 2007). Why? A couple of explanations are conceivable. First, mutant SOD1 transgenic mice may not be a good model for human sporadic ALS cases despite their apparent similarities. Indeed, mutant SOD1 associated FALS and SALS exhibit different microscopic neuropathology. The former is characterized by Lewy body-like inclusion containing mutant SOD1, whereas for the latter skein-like or round inclusions containing TDP-43. Since TDP-43 is implicated in the pathogenesis of SALS as well as in a subgroup of FALS, developing a new ALS mouse model based on TDP-43 could solve these problems in the future (Neumann et al., 2007). A second possible explanation is that the most therapies in mouse models are initiated prior to disease onset, which is impossible in human patients until presymptomatic diagnosis for ALS becomes available. Thirdly, whether drug dosage and bioavailablity comparable to mouse experiments are replicated in human trials remains unclear.

An alternative explanation is the difference in the design of mouse experimental therapies and human clinical trials. Randomized controlled trials, which are designed to eliminate numerous confounding factors including observation biases, are standard in human clinical trials. In contrast, mouse experiments are generally not performed as rigorously as human trials, increasing risks of producing "false positive" results (Benatar, 2007).

Edaravone (3-methyl-1-phenyl-2-pyrazolin-5-one) is a free radical scavenger that has been approved in Japan since 2001 as a therapeutic agent to reduce neuronal damage caused by acute ischemic stroke (Yoshida et al., 2006). Edaravone eliminates lipid peroxide and hydroxyl radicals by transferring an electron to the radical, thereby ameliorating the ischemic neuronal damage. Oxidative stress is implicated as one of the pathogenetic mechanisms for ALS (Barber et al., 2006). Moreover, a small-sized open trial of edaravone suggested that edaravone is safe and may delay the progression of functional motor disturbances in ALS patients (Yoshino and Kimura, 2006). Thus, edaravone is a promising therapeutic agent for human motor neuron diseases including ALS.

In a previous issue, Ito et al. reported an experimental therapy of a mutant SOD1 mouse model using edaravone (Ito et al., 2008). Taking the problems associated with the therapeutic experimental design in mouse experiments, they carefully optimized the dosage of edaravone so that the pharmacokinetic profile after intraperitoneal injection became comparable to that in human patients. Moreover, they started treatment only after the disease onset, similar to human ALS treatment. Furthermore, they used only female mice for analysis considering the gender difference in lifespan and randomized blind analyses were adopted for all the behavioral as well as pathological observations. This methodological rigorousness has never been considered seriously in previous experimental therapies of mutant SOD1 ALS mouse models, most of which have failed to be replicated in human patients.

Edaravone significantly slowed the motor function decline as assessed by multiple behavioral tests such as rotarod tests. However, the lifespan of edaravone-treated mice were not significantly higher

* Fax: +81 75 761 9780.
E-mail address: ryosuket@kuhp.kyoto-u.ac.jp.

0014-4886/$ - see front matter
doi:10.1016/j.expneurol.2009.03.001

than those of control mice, suggesting that edaravone may improve the motor function of the ALS mice without apparent lifespan expanding effects (Ito et al., 2008). This uncoupling in the mechanisms underlying motor function and lifespan further implies that pathways causing motor function decline are not necessarily the ones causing eventual death, usually by respiratory muscle failure. That said, it would be possible to identify drugs that can improve the quality of life in ALS patients without affecting lifespan, which seems to be an easier goal compared with identifying lifespan-extending drugs for ALS. Moreover, it was clinically important that edaravone was effective even when administered after the disease onset. On the other hand, it would be intriguing to administer edaravone to ALS mice at their presymptomatic stage to understand how the point at which edaravone is used during the course of disease affects its outcome.

It is noted that high-dose edaravone treatment leads to a decrease of mutant SOD1 accumulation in the spinal cord. Since administration of edaravone resulted in a marked decrease of 3-nitrotyrosine/tyrosine ratio, a marker of oxidative stress, suppression of oxidative stress is likely to be upstream of the inhibition of aggregate formation (Kabashi and Durham, 2006; Valentine and Hart, 2003). It has long been debated how oxidative stress is induced by SOD1 mutations (Barber et al., 2006). Reduced enzymatic activity of SOD1 and generation of peroxynitrite due to aberrant copper chemistry have been proposed as plausible mechanism explaining "gain of toxic function" of mutant SOD1 (Beckman et al., 1993; Deng et al., 1993; Robberecht et al., 1994). However, the fact that a subgroup of SOD1 mutants retains full enzymatic activity and that H46R and H48Q mutants which completely lose binding sites for copper still cause ALS suggests that mechanisms unrelated to SOD1 activity may also be involved (Borchelt et al., 1994; Valentine et al., 2005; Wang et al., 2003). It has been shown that mutant SOD1 overexpression in a neuronal cell line leads to transcriptional repression of antioxidant proteins by reducing the level of transcriptional factor NRF2 (Kirby et al., 2005). It would be intriguing to investigate whether edaravone affects the level of NRF2 when administered to ALS mice.

Another interesting unresolved question is which cells are the targets of edaravone. Recently, it has been shown that motor neuron death in mutant SOD1 ALS mouse models is non-cell autonomous (Boillee et al., 2006; Yamanaka et al., 2008). In other words, mutant SOD1-expressing astroglial or miroglial cells promote motor neuron death. In this context, edarovone may decrease the aggregates in non-neuronal glial cells, resulting in amelioration of neurodegeneration. These questions should be addressed in further analysis in the future.

A recent systematic review of randomized controlled trials of antioxidant therapies against ALS including vitamin E and acetylcysteine has shown that there is no substantial evidence to support their clinical use (Orrell et al., 2008). However, the evidence for the beneficial effects of edaravone on human ALS patients awaits the publication of the results of a phase III clinical trial of ALS, currently ongoing in Japan (http://www.als.net/research/studies/tdfAnimalStudyList.asp).

Acknowledgment

I thank Roberto Gavinio for kindly editing this manuscript.

References

Barber, S.C., Mead, R.J., Shaw, P.J., 2006. Oxidative stress in ALS: a mechanism of neurodegeneration and a therapeutic target. Biochim. Biophys. Acta 1762, 1051–1067.
Beckman, J.S., Carson, M., Smith, C.D., Koppenol, W.H., 1993. ALS, SOD and peroxynitrite. Nature 364, 584.
Benatar, M., 2007. Lost in translation: treatment trials in the SOD1 mouse and in human ALS. Neurobiol. Dis. 26, 1–13.
Boillee, S., Yamanaka, K., Lobsiger, C.S., Copeland, N.G., Jenkins, N.A., Kassiotis, G., Kollias, G., Cleveland, D.W., 2006. Onset and progression in inherited ALS determined by motor neurons and microglia. Science 312, 1389–1392.
Borchelt, D.R., Lee, M.K., Slunt, H.S., Guarnieri, M., Xu, Z.S., Wong, P.C., Brown Jr., R.H., Price, D.L., Sisodia, S.S., Cleveland, D.W., 1994. Superoxide dismutase 1 with mutations linked to familial amyotrophic lateral sclerosis possesses significant activity. Proc. Natl. Acad. Sci. U. S. A. 91, 8292–8296.
Deng, H.X., Hentati, A., Tainer, J.A., Iqbal, Z., Cayabyab, A., Hung, W.Y., Getzoff, E.D., Hu, P., Herzfeldt, B., Roos, R.P., et al., 1993. Amyotrophic lateral sclerosis and structural defects in Cu,Zn superoxide dismutase. Science 261, 1047–1051.
Gurney, M.E., Pu, H., Chiu, A.Y., Dal Canto, M.C., Polchow, C.Y., Alexander, D.D., Caliendo, J., Hentati, A., Kwon, Y.W., Deng, H.X., et al., 1994. Motor neuron degeneration in mice that express a human Cu,Zn superoxide dismutase mutation. Science 264, 1772–1775.
Ito, H., Wate, R., Zhang, J., Ohnishi, S., Kaneko, S., Ito, H., Nakano, S., Kusaka, H., 2008. Treatment with edaravone, initiated at symptom onset, slows motor decline and decreases SOD1 deposition in ALS mice. Exp. Neurol. 213, 448–455.
Kabashi, E., Durham, H.D., 2006. Failure of protein quality control in amyotrophic lateral sclerosis. Biochim. Biophys. Acta 1762, 1038–1050.
Kirby, J., Halligan, E., Baptista, M.J., Allen, S., Heath, P.R., Holden, H., Barber, S.C., Loynes, C.A., Wood-Allum, C.A., Lunec, J., Shaw, P.J., 2005. Mutant SOD1 alters the motor neuronal transcriptome: implications for familial ALS. Brain 128, 1686–1706.
Mitchell, J.D., Borasio, G.D., 2007. Amyotrophic lateral sclerosis. Lancet 369, 2031–2041.
Neumann, M., Kwong, L.K., Sampathu, D.M., Trojanowski, J.Q., Lee, V.M., 2007. TDP-43 proteinopathy in frontotemporal lobar degeneration and amyotrophic lateral sclerosis: protein misfolding diseases without amyloidosis. Arch. Neurol. 64, 1388–1394.
Orrell, R.W., Lane, R.J., Ross, M., 2008. A systematic review of antioxidant treatment for amyotrophic lateral sclerosis/motor neuron disease. Amyotroph. Lateral Scler. 9, 195–211.
Robberecht, W., Sapp, P., Viaene, M.K., Rosen, D., McKenna-Yasek, D., Haines, J., Horvitz, R., Theys, P., Brown Jr., R., 1994. Cu/Zn superoxide dismutase activity in familial and sporadic amyotrophic lateral sclerosis. J. Neurochem. 62, 384–387.
Rosen, D.R., Siddique, T., Patterson, D., Figlewicz, D.A., Sapp, P., Hentati, A., Donaldson, D., Goto, J., O'Regan, J.P., Deng, H.X., et al., 1993. Mutations in Cu/Zn superoxide dismutase gene are associated with familial amyotrophic lateral sclerosis. Nature 362, 59–62.
Valentine, J.S., Hart, P.J., 2003. Misfolded CuZnSOD and amyotrophic lateral sclerosis. Proc. Natl. Acad. Sci. U. S. A. 100, 3617–3622.
Valentine, J.S., Doucette, P.A., Zittin Potter, S., 2005. Copper-zinc superoxide dismutase and amyotrophic lateral sclerosis. Annu. Rev. Biochem. 74, 563–593.
Wang, J., Slunt, H., Gonzales, V., Fromholt, D., Coonfield, M., Copeland, N.G., Jenkins, N.A., Borchelt, D.R., 2003. Copper-binding-site-null SOD1 causes ALS in transgenic mice: aggregates of non-native SOD1 delineate a common feature. Hum. Mol. Genet. 12, 2753–2764.
Yamanaka, K., Chun, S.J., Boillee, S., Fujimori-Tonou, N., Yamashita, H., Gutmann, D.H., Takahashi, R., Misawa, H., Cleveland, D.W., 2008. Astrocytes as determinants of disease progression in inherited amyotrophic lateral sclerosis. Nat. Neurosci. 11, 251–253.
Yoshida, H., Yanai, H., Namiki, Y., Fukatsu-Sasaki, K., Furutani, N., Tada, N., 2006. Neuroprotective effects of edaravone: a novel free radical scavenger in cerebrovascular injury. CNS Drug Rev. 12, 9–20.
Yoshino, H., Kimura, A., 2006. Investigation of the therapeutic effects of edaravone, a free radical scavenger, on amyotrophic lateral sclerosis (Phase II study). Amyotroph. Lateral. Scler. 7, 241–245.

Journal of Neuroscience Research 87:576–585 (2009)

Nicotinic Receptor Stimulation Protects Nigral Dopaminergic Neurons in Rotenone-induced Parkinson's Disease Models

Hiroki Takeuchi,[1] Takashi Yanagida,[2] Masatoshi Inden,[2] Kazuyuki Takata,[2] Yoshihisa Kitamura,[2] Kentaro Yamakawa,[3] Hideyuki Sawada,[3] Yasuhiko Izumi,[4] Noriyuki Yamamoto,[4] Takeshi Kihara,[4] Kengo Uemura,[1] Haruhisa Inoue,[1] Takashi Taniguchi,[2] Akinori Akaike,[4] Ryosuke Takahashi,[1] and Shun Shimohama[5]*

[1]Department of Neurology, Graduate School of Medicine, Kyoto University, Kyoto, Japan
[2]Department of Neurobiology, Kyoto Pharmaceutical University, Kyoto, Japan
[3]Clinical Research Center, National Hospital Organization Utano National Hospital, Kyoto, Japan
[4]Department of Pharmacology, Graduate School of Pharmaceutical Sciences, Kyoto University, Kyoto, Japan
[5]Department of Neurology, Sapporo Medical University, Sapporo, Japan

Parkinson's disease (PD) is the second most common neurodegenerative disease and is characterized by dopaminergic (DA) neuronal cell loss in the substantia nigra. Although the entire pathogenesis of PD is still unclear, both environmental and genetic factors contribute to neurodegeneration. Epidemiologic studies show that prevalence of PD is lower in smokers than in nonsmokers,. Nicotine, a releaser of dopamine from DA neurons, is one of the candidates of antiparkinson agents in tobacco. To assess the protective effect of nicotine against rotenone-induced DA neuronal cell toxicity, we examined the neuroprotective effects of nicotine in rotenone-induced PD models in vivo and in vitro. We observed that simultaneous subcutaneous administration of nicotine inhibited both motor deficits and DA neuronal cell loss in the substantia nigra of rotenone-treated mice. Next, we analyzed the molecular mechanisms of DA neuroprotective effect of nicotine against rotenone-induced toxicity with primary DA neuronal culture. We found that DA neuroprotective effects of nicotine were inhibited by dihydro-β-erythroidine (DHβE), α-bungarotoxin (αBuTx), and/or PI3K-Akt/PKB (protein serine/threonine kinase B) inhibitors, demonstrating that rotenone-toxicity on DA neurons are inhibited via activation of α4β2 or α7 nAChRs-PI3K-Akt/PKB pathway or pathways. These results suggest that the rotenone mouse model may be useful for assessing candidate antiparkinson agents, and that nAChR (nicotinic acetylcholine receptor) stimulation can protect DA neurons against degeneration. © 2008 Wiley-Liss, Inc.

Key words: Parkinson's disease; rotenone; nicotine; dopaminergic neuron; neuroprotection

Parkinson's disease (PD) is the second most common progressive neurodegenerative disorder. It is characterized by relatively selective degeneration of dopaminergic neurons in the substantia nigra and loss of dopamine in the striatum resulting in resting tremor, rigidity, bradykinesia and postural instability (Dunnett and Björklund, 1999; Shimohama et al., 2003). Although the pathogenesis of PD is still unclear, it is thought that both environmental and genetic factors cause neurodegeneration. Rural residency, pesticides and intrinsic toxic agents were reported as environmental risk factors for sporadic PD. Recent studies revealed several mutations in familial PD genes such as α-synuclein, parkin, PINK1, LRRK2 (leucine-rich repeat kinase 2), DJ-1, and UCH-L1 (ubiquitin C-terminal hydrolase-L1) (Schapira, 2006). Epidemiological studies suggest that the use of pesticides increases the risk of PD, possibly via reduced activity of complex I in the mitochondrial respiratory chain in the substantia nigra and result in the pathogenesis of PD (Parker et al., 1989; Mann et al., 1992; Mizuno et al., 1998). 6-hydroxydopamine (6-OHDA), a H_2O_2 pro-oxidant and 1-methyl-4-phenyl-1,2,3,6-tetrahydropyridine (MPTP), a mitochondrial complex I inhibitor, have been widely used to produce toxin models of sporadic PD. Chronic exposure to rotenone, a nature-derived pesticide, could be a more

*Correspondence to: Shun Shimohama, MD, PhD, Department of Neurology, Sapporo Medical University, S1W17, Chuo-ku, Sapporo, 060-8556, Japan. E-mail: shimoha@sapmed.ac.jp

Received 18 March 2008; Revised 28 May 2008; Accepted 13 July 2008

Published online 19 September 2008 in Wiley InterScience (www.interscience.wiley.com). DOI: 10.1002/jnr.21869

appropriate animal PD model because rotenone-treated animals show slowly progressive DA neuronal loss, and Lewy body–like particles, which are primarily aggregations of α-synuclein (Betarbet et al., 2000, Inden et al., 2007).

On the other hand, current drug therapy is limited to supplementing dopamine (DA) or enhancing dopaminergic effect. Some may have neuroprotective effects, but their effects remain controversial (Quik, 2004; Du et al., 2005; Iravani et al., 2006). It has also been reported that smokers have a lower risk for PD (De Reuck et al., 2005; Wirdefeldt et al., 2005), and nAChRs (nicotinic acetylcholine receptor) were decreased in the brains of PD patients (Fujita et al., 2006) and PD model animals (Quik et al., 2006). Nicotine may up-regulate DA release at striatum from nigral dopaminergic neurons (Morens et al., 1995), followed by stimulation of α4β2 nAChRs (Champtiaux et al., 2003). Furthermore, nicotine could protect mitochondria and had protective effect from oxidative stress (Cormier et al., 2003; Xie et al., 2005). In studies made in vivo, stimulation of nAChRs resulted in neuroprotection in cerebral ischemia and PD model animals (Shimohama et al., 1998; Kagitani et al., 2000; Parain et al., 2003). In vitro, we have demonstrated that nicotine protected rat cortical neurons against glutamate toxicity and lower motor neurons against β-amyloid toxicity respectively, and that nicotine was antiapoptotic (Akaike et al., 1994; Kihara et al., 1997, 2001; Nakamizo et al., 2005). Also nicotine protected rat nigral dopaminergic neurons against 1-methyl-4-phenylpyridinium (MPP^+) cytotoxicity by non-α7 nAChR stimulation (Jeyarasasingam et al., 2002). So nicotinic receptor stimulation may be a good target for DA neuroprotective therapy toward PD. However, the further protective mechanisms for dopaminergic neurons have not been elucidated.

In this study, we investigated the neuroprotective effect of nicotine against nigral DA neuronal death induced by rotenone with a chronic rotenone-treated PD mouse model, and analyzed molecular mechanisms of the protection in dissociated cultures of the fetal rat ventral mesencephalon.

MATERIALS AND METHODS

Materials

Rotenone, (−)-nicotine hydrogen bitartrate, mecamylamine (Mec), αBuTx, DHβE, and triciribine, an Akt/PKB inhibitor, were purchased from Sigma (St. Louis, MO). LY294002, a PI3K (phosphatidylinositol 3-kinase) inhibitor was from Calbiochem (Darmstadt, Germany). Carboxylmethyl cellulose (CMC) was obtained from Nacalai Tesque (Kyoto, Japan). Mouse monoclonal antibodies against microtubule-associated protein 2 (MAP2), tyrosine hydroxylase (TH) and β-actin were purchased from Sigma. Rabbit polyclonal antibody against TH was from Chemicon (Temecula, CA).

Mouse Model and Drug Administration

Eight-week-old male C57BL/6J mice (20–25 g) were purchased from Japan SLC Inc. (Hamamatsu, Japan). The animals were acclimated and maintained at 23°C under a 12-hr light/dark cycle (lights on 09.00–21.00 hr). Mice were housed in standard laboratory cages and had free access to food and water throughout the study period. All animal experiments were carried out in accordance with the National Institutes of Health (NIH) Guide for the Care and Use of Laboratory Animals, and the protocols were approved by the Committee for Animal Research at Kyoto University. Rotenone was administrated orally once daily by gavage with a catheter at a dose of 30 mg/kg for 28 days. Rotenone was suspended in 0.5% CMC and administrated orally once daily at a concentration of 12 mL/kg body weight. The 0.5% CMC was administrated orally as vehicle to control mice (Inden et al., 2007). For in vivo experiments, nicotine ((−)-nicotine hydrogen bitartrate dissolved in saline) at a dose of 0.21 or 0.42 mg/kg (free base) was daily injected subcutaneously at 30 min before each oral administration of rotenone. Saline was injected in parallel as the corresponding vehicle control. Each group contained 6–12 mice.

Behavior Analysis

The behavior of each mouse was assessed by the rotarod treadmill test. The rotarod treadmill (accelerating model 7750, Ugo Basile, Varese, Italy) consists of a plastic rod, 6 cm in diameter and 36 cm long, with a nonslippery surface 20 cm above the base (trip plate). This rod is divided into four equal sections by five discs (25 cm in diameter), which enables four mice to walk on the rod at the same time. In the present study, the accelerating rotor mode was used (10-grade speeds from 3.5 to 35 r.p.m. for 5 min). Time was recorded while mice were running on the rod (from when they were put on the rod to when they fell off).

Immunohistochemistry

Mice were perfused with 10 mM phosphate-buffered saline (PBS) and then 4% paraformaldehyde in 100 mM phosphate buffer (PB) under deep anesthesia with pentobarbital (100 mg/kg, intraperitoneal injection). After perfusion, the brain was quickly removed and postfixed for 2 days and then transferred to 15% sucrose solution in 100 mM PB at 4°C at least for 4 days. After cryoprotection, the brain was rapidly frozen by heat exchange from vaporized CO_2 gas (−70°C) and then sections (60 μm) were cut with a cryostat and collected in 100 mM PBS containing 0.3% Triton X-100 (PBS-T). After several washes, the sections were stored until use in a free-floating state at 4°C for immunohistochemical analysis.

Brain sections were incubated with primary rabbit polyclonal antibody to TH (1:10,000), for 3 days at 4°C, and next with biotinylated antibody to rabbit IgG (1:2000) for 2 hr at room temperature. Then the sections were incubated with avidin peroxidase (1:4000) with the ABC kit for 1 hr at room temperature. All sections were rinsed several times with PBS-T between incubations. Labeling was revealed by DAB (3-3′-diaminobenzidine tetrahydrochloride) with nickel ammonium, which yielded a dark blue color.

Stereological Analysis

The total number of dopaminergic neurons in both hemispheres of the substantia nigra pars compacta (SNC) was